



# Specific heat investigation of bulk metallic glasses

**A. Januszka\*, R. Nowosielski**

Division of Nanocrystalline and Functional Materials and Sustainable  
Pro-ecological Technologies, Institute of Engineering Materials and Biomaterials,  
Silesian University of Technology, ul. Konarskiego 18a, 44-100 Gliwice, Poland

\* Corresponding e-mail address: anna.januszka@polsl.pl

Received 19.10.2013; published in revised form 01.12.2013

## ABSTRACT

**Purpose:** The aim of the paper is measurements and analysis of specific heat ( $C_p$ ) of bulk metallic glasses. The fabrication method and structure analysis were also described.

**Design/methodology/approach:** The studies were carried out on FeCo-based glassy test pieces with the following composition:  $Fe_{36}Co_{36}B_{19.2}Si_4$ . Samples in form of rods were prepared by copper mould casting method. The structure was tested by X-ray diffraction method and scanning electron microscope observation (SEM). For determination of thermal properties the DTA and DSC method were used. Specific heat of amorphous samples was investigated by calorimetric method.

**Findings:** The X-ray diffraction revealed that fabricated samples exhibit glassy structure. Broad diffraction halo could be seen for each tested sample. SEM observations show that fracture morphology is changed on the diameter of samples. Thermal analysis allows assigning liquidus temperature ( $T_l$ ). On the base of DSC curves glass transition temperature ( $T_g$ ) and crystallization temperature ( $T_x$ ) were determinate. Specific heat investigation show insignificant changes in temperature range from 30 K to  $T_g$ .

**Practical implications:** Bulk glassy FeCo-based alloys which are fabricated by rapidly solidifying technique are very interesting engineering materials because of its unique mechanical and magnetic properties. They could be used in many applications. Specific heat is important in solidification process. This property is significant input-data in computer simulation of solidification process.

**Originality/value:** It is important to investigate thermal properties of bulk metallic glasses (including  $C_p$ ) in order to understand mechanism of structural relaxation, glass transition and crystallization sequences.

**Keywords:** Specific heat; Thermal properties; Amorphous materials; Metallic glasses; FeCo-based alloys

**Reference to this paper should be given in the following way:**

A. Januszka, R. Nowosielski, Specific heat investigation of bulk metallic glasses, Archives of Materials Science and Engineering 64/2 (2013) 144-151.

## PROPERTIES

### 1. Introduction

In our life materials are diverse and have many differently uses. Great number of metals, ceramics, polymers, composites and the other engineering materials applications are based on their unique thermo-physical properties. Among them it could be distinguished specific heat, thermal conductivity and thermal expansion. This properties, largely, depends on chemical

composition and structure of material. They also depend on temperature.

Metallic glasses, as a newcomer engineering materials are investigated for the sake of thermal properties. A various metallic glasses have been developed during last 50 years. They are classified into metal-metalloid or metal-metal type although other classification also existing (Table 1) [1-6]. Among bulk metallic glasses Fe-based alloy plays significant role. The unique properties

of these materials allow using them in many engineering applications.

During fabrication of metallic glasses it is necessary to cooling rate will be high enough. For metallic glasses which belong to group so-called “conventional” metallic glasses cooling rate reach  $10^3$ - $10^6$  K/s but for group “bulk metallic glasses” cooling rate decrease, and it should equal  $10^3$  K/s or less. Bulk metallic glasses exhibit very good glass forming ability which is comparable to glass forming ability of silica glass. In dependence on chemical composition it is possible to obtain this material with dimension even 100 mm [7-15].

Table 1.  
Classification of bulk metallic glasses composition [14,15]

Group	Chemical elements of bulk metallic glasses		Example
	Main components	Others components	
I	Transition metal of IV to VI group of periodic table (ETM) or lanthanides (Ln)	Al, Ga, Sn and transition metal of VII to VIII group of periodic table (LTM)	Zr-Al-Ni, Zr-Nb-Al-Ni-Ln
II	Transition metal of IV to VI group of periodic table (ETM) or lanthanides (Ln)	Transition metal of VII to VIII group of periodic table (LTM) and non-metallic element (NM)	Fe-Zr-B, Co-Zr-Nb-B
III	Transition metal of VII to VIII group of periodic table (LTM)	Al, Ga, Sn and non-metallic element (NM)	Fe-(Al,Ga)-NM
IV	Mg or Be with transition metal of VII to VIII group of periodic table (LTM) or lanthanides (Ln)	Transition metal of IV to VI group of periodic table (ETM)	Mg-Ln-Ni, Zr-Ti-Be-Ni-Cu
V	Transition metal of VII to VIII group of periodic table (LTM)	Non-metallic element (NM)	Pd-Ni-P, Pt-Ni-P

Cooling time from liquidus temperature which allows obtaining sample with amorphous structure in whole section should equal  $\tau$  (1) [7, 16]:

$$\tau = \frac{D^2}{k} \quad (1)$$

where:

D - sample dimension [mm],  
k - thermal diffusivity.

Thermal diffusivity is described by formula 2, where  $\lambda$  is thermal conductivity [W/mK] and  $C_p$  is specific heat [J/gK] [7, 16-20].

$$k = \frac{\lambda}{C_p} \quad (2)$$

The specific heat ( $C_p$ ) of a substance is a property that relates the temperature and the heat of an object. It is defined as a quantity of heat required to rise one gram of a substance by  $1^\circ\text{C}$ . It can be expressed in units [J/g\* $^\circ\text{C}$ , cal/ g\*  $^\circ\text{C}$  or J/mol\*  $^\circ\text{C}$ ]. The relationship between heat (q), specific heat ( $C_p$ ), mass (m) and change of temperature ( $\Delta T$ ) could be written in the form of equation 3 [7, 16]:

$$q = m \cdot C_p \cdot \Delta T \quad (3)$$

Where change of temperature  $\Delta T$  it is a difference between final temperature ( $T_f$ ) and initial temperature ( $T_i$ ) of an object. Table 2 presents specific heat of few chosen materials.

Table 2.  
Specific heat of several substances [21]

Substance	Specific heat [J/g* $^\circ\text{C}$ ]
air	1.05
aluminium	0.899
alcohol	2.4
carbon dioxide	0.841
copper	0.385
glass	0.500
iron	0.448
lead	0.129
nickel	0.444
silver	0.24
tin	0.222
water	4.184
wood	1.8
zinc	0.385

During transition of liquid metal/alloy to glass form variation, or rather oscillation, of specific heat ( $C_p$ ) could be observed (Fig. 1).

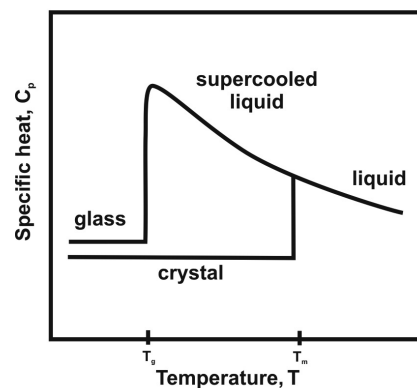


Fig. 1. Variation of specific heat with temperature for glass and crystal formation [7]

With temperature decrease, up to  $T_g$ , specific heat of supercooled liquid slowly increases. In glass transition temperature it could be noticed drastic decrease of specific heat. This indicates that metal/alloy was freezing and takes the glassy structure.

Knowledge about specific heat of metallic glasses at the glass transition region is meaningful to understand the mechanism for the structural relaxation, the glass transition and crystallization sequences in this materials. Cooling rate during vitrification process has a significant influence on the glass transition temperature ( $T_g$ ) [18].  $T_g$  can be determined by DSC measurements during sample heating. This research method allow to also specific heat evaluation. Usually it is calculating by computer software, which uses relationship between specific heat of measured sample and specific heat of standard sample.

In this paper authors presented differential scanning calorimetry (DSC) measurements of the specific heat. Results are presented as a function of temperature.

## 2. Materials and method

### 2.1. Studied material

The investigated material was cast in form of rods with diameter of 2 mm. Before casting process, master alloy must have been fabricated. Pure chemical elements (Fig. 3, Table 3) were melted by induction heater in argon atmosphere. The ingot was melted several times in order to obtaining homogeneity. Table 4 present chemical composition of Fe-Co-B-Si-Nb alloy in detail.

Table 3.  
Shape and purity of chemical elements

Elements	Shape	Purity [%]
Fe	solid particles	99.75
Co	flat solid particles	99.89
B	pieces	99.9
Si	pieces	99.9
Nb	powder	99.85

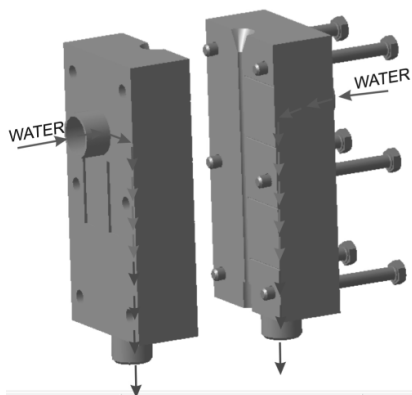


Fig. 2. Pressure-casting die

After master alloy mechanical purify it was put into quartz crucible. Next, it was melted by induction coil and insert into copper mould (Fig. 4) using argon pressure. Copper mould was additionally cooled by water (Fig. 2). Thanks to this cooling matter require cooling rate of liquid alloy could be obtained.

Table 4.  
Chemical composition of Fe-Co-B-Si-Nb

Elements	at. [%]	mass. [%]
Fe	36.00	41.53
Co	36.00	43.83
B	19.20	4.29
Si	4.80	2.67
Nb	4.00	7.68

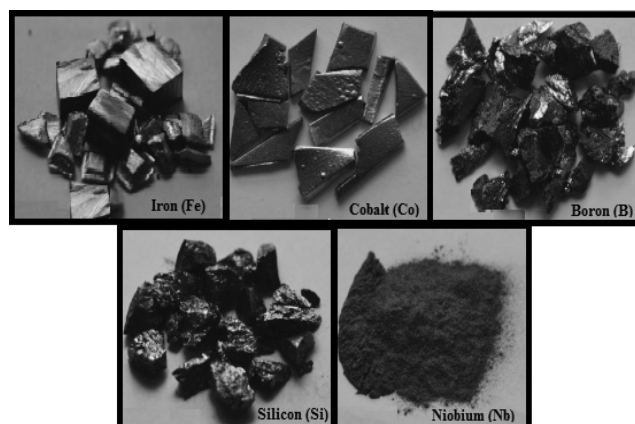


Fig. 3. Shapes of chemical elements

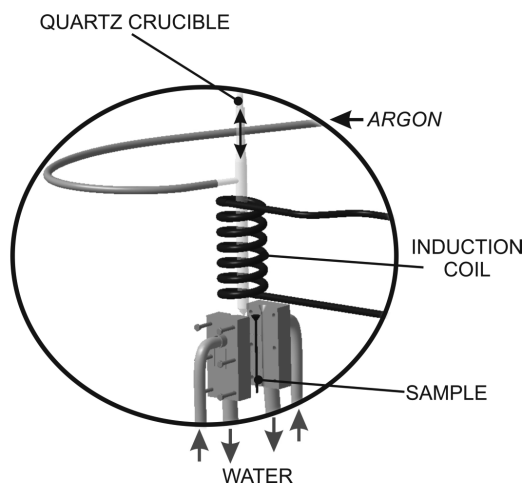


Fig. 4. Scheme of casting process

Within a framework of investigation, the bulk samples in form of rods with diameter of 2 mm were fabricated (Fig. 5). In this paper there are results of analyses for five samples with the same diameter.

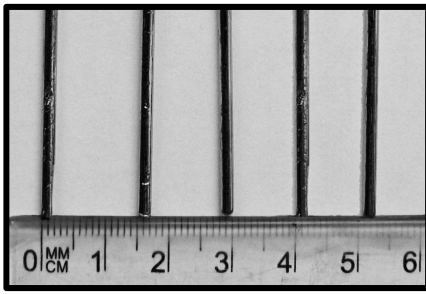


Fig. 5 Outer morphology of glassy  $\text{Fe}_{36}\text{Co}_{36}\text{B}_{19.2}\text{Si}_{4.8}\text{Nb}_4$  rods with diameter 2mm in as-cast state

## 2.2. Research methodology

The melting point temperature ( $T_m$ ) and liquidus temperature ( $T_l$ ) of  $\text{Fe}_{36}\text{Co}_{36}\text{B}_{19.2}\text{Si}_{4.8}\text{Nb}_4$  master alloy was determined by differential thermal analysis (DTA). The heating rate of DTA measurements was 10 K/min in the temperature range of 300 to 1700 K.

Structure analysis of studied rods in as-cast state was carried out by X-ray diffraction using Phillips X'Pert diffractometer with  $\text{Co K}\alpha$  radiation at 20 kV. The diffraction lines were recorded by means of the stepwise method within the angular range of  $20^\circ$  to  $120^\circ$ .

Thermal stability including the glass transition temperature ( $T_g$ ), supercooled liquid region, the onset crystallization temperature ( $T_x$ ) and peak crystallization temperature ( $T_p$ ) were examined by differential scanning calorimetry (DSC). DSC investigations were carried out in the temperature range of 300 to 1200 K.

Specific heat of glassy rods with diameter of 2 mm was measured by calorimetric method. Measurements of specific heat were carried out on the base of international standard ISO-11357-4. Tests were realized by comparative method. In this method results of specific heat are comparing with material with known properties. In this case the standard sample was sapphire. Specific heat was calculated by computer temperature program in accordance the formula 4:

$$C_p = C_{p\_sapphire} \cdot \left( \frac{HF \cdot m_{sapphire}}{m \cdot HF_{sapphire}} \right) \quad (4)$$

were:

$C_p$  - specific heat [J/gK],  
 HF - heat flow [dQ/dt],  
 m - mass of sample [g].

Microscope observations of fracture morphology were realized using Zeiss Supra 25 scanning electron microscope. SEM micrographs were carried out with different magnification.

## 3. Results and discussion

Differential thermal analysis allow to identification the solidus and liquidus temperature. Sharply outlined one

endothermic peak (Fig. 6) indicates the eutectic chemical composition of prepared master alloy. Melting process has been started in 1350 K and on the curve it is marked as  $T_m$ . Liquidus temperature ( $T_l$ ) equal 1434 K.

The XRD investigation confirmed that the rods in diameter of 2 mm with chemical composition of  $\text{Fe}_{36}\text{Co}_{36}\text{B}_{19.2}\text{Si}_{4.8}\text{Nb}_4$  exhibit amorphous state. One broad peak which is characteristic for amorphous structure (Fig. 7).

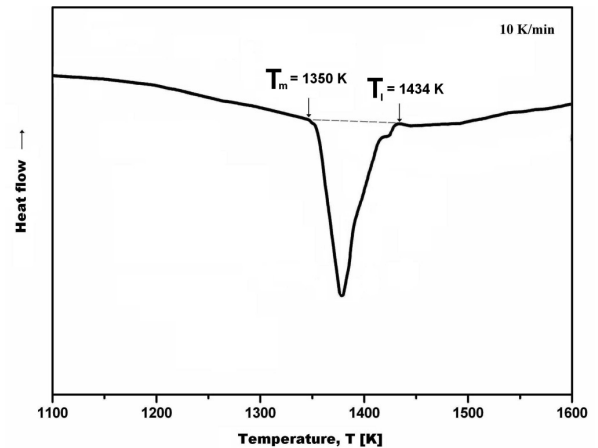


Fig. 6. DTA curve of master alloy

The DSC curves (10 K/min) obtained for glassy rods with diameter of 2 mm are shown in Fig. 8. Results of DSC investigation of studied samples enable evaluate of glass transition temperature, onset ( $T_x$ ) and peak crystallization temperature ( $T_p$ ).

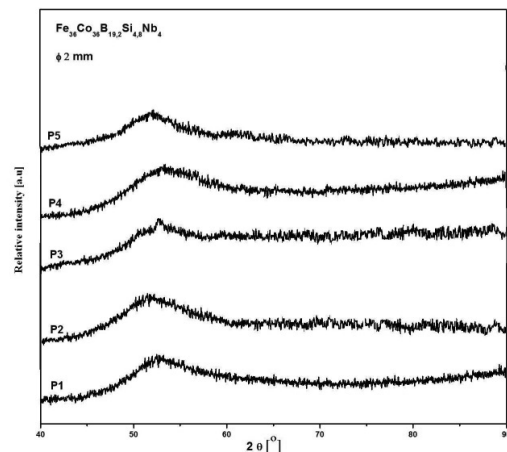


Fig. 7. X-ray diffraction patterns of  $\text{Fe}_{36}\text{Co}_{36}\text{B}_{19.2}\text{Si}_{4.8}\text{Nb}_4$  glassy rods with diameter of  $\phi = 2$  mm in as-cast state

Glass transition temperature equal 805 and 806 K adequately. The crystallization effect is describing by one exothermic peak and indicate onset crystallization temperature ( $T_x$ ) in 840 and 842 K, while peak crystallization temperature ( $T_p$ ) is equal 35 and 36 K adequately.

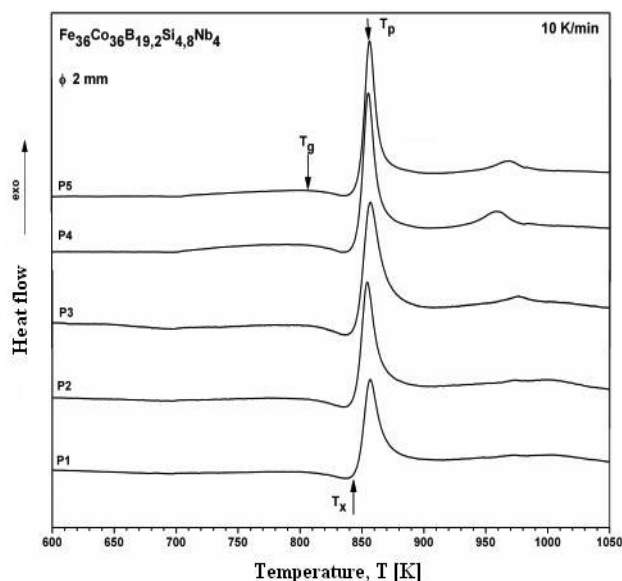


Fig. 8. DSC curves of  $\text{Fe}_{36}\text{Co}_{36}\text{B}_{19.2}\text{Si}_{4.8}\text{Nb}_4$  glassy rods with diameter of 2 mm.

Additionally, on the base of DSC measurements typical parameters which are important from the point of view of glass forming ability were calculated. It enclose supercooled liquid region ( $\Delta T_x$ ), reduced glass transition temperature ( $T_{rg}$ ) and GFA parameters such as  $\alpha$ ,  $\beta$ ,  $\gamma$ . The GFA parameters were calculated based on [2, 5, 7, 8] (Table 5).

Table 5.

Thermal properties and selected GFA parameters of glassy rods with diameter of 2 mm

Parameters	Sample				
	P1	P2	P3	P4	P5
$T_l$ [K]	1434				
$T_g$ [K]	806	805	805	806	806
$T_x$ [K]	842	840	840	842	842
$T_p$ [K]	856	854	856	856	856
$\Delta T_x$ [K]	36	35	35	36	36
$T_{rg}$ [K]	0.562	0.561	0.561	0.562	0.562
$\alpha$	0.587	0.585	0.585	0.587	0.587
$\beta$	1.607	1.604	1.604	1.607	1.607
$\gamma$	0.376	0.375	0.375	0.376	0.376

Specific heat ( $C_p$ ) measurements were realized with heating rate 10 K/min. Figs. 9-13 presents results of  $C_p$  investigations. Analysis of the  $C_p$  was carried out in the temperature range of 300 to 1000 K. As it can be observed, all of tested samples exhibit comparable specific heat values. In the temperature range of 400 K to  $T_g$   $C_p$  is change in a small range and it average 0,829 ( $\pm 0,115$ ) J/g\*K for P1, 0,743 ( $\pm 0,091$ ) J/g\*K for P2, 0,737 ( $\pm 0,082$ ) J/g\*K for P3, 0,637 ( $\pm 0,064$ ) J/g\*K for P4 and 0,603 ( $\pm 0,050$ ) J/g\*K for P5. Figure 14 presents mean errors of specific heat measurements.

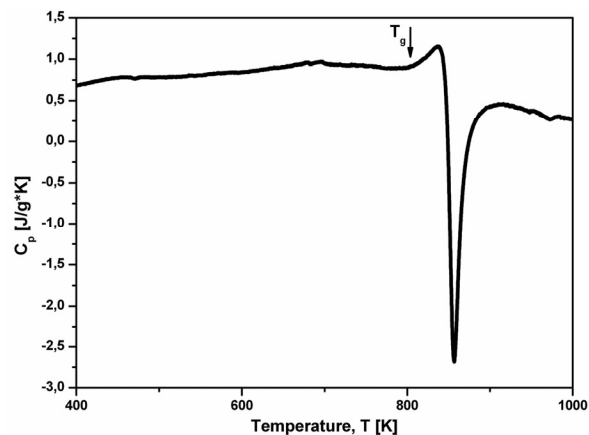


Fig. 9. The specific heat of  $\text{Fe}_{36}\text{Co}_{36}\text{B}_{19.2}\text{Si}_{4.8}\text{Nb}_4$  in form of rods with diameter of 2 mm in as-cast state (sample P1)

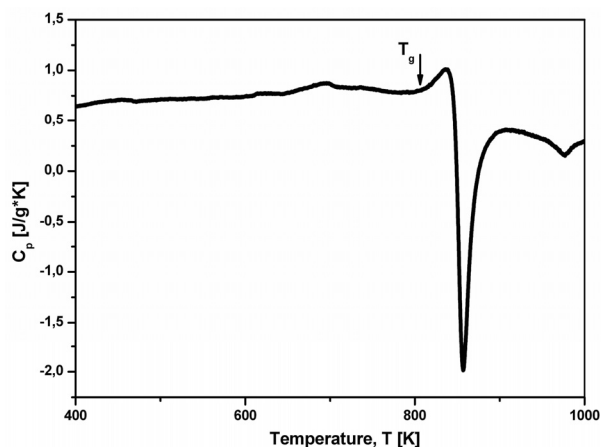


Fig. 10. The specific heat of  $\text{Fe}_{36}\text{Co}_{36}\text{B}_{19.2}\text{Si}_{4.8}\text{Nb}_4$  in form of rods with diameter of 2 mm in as-cast state (sample P2)

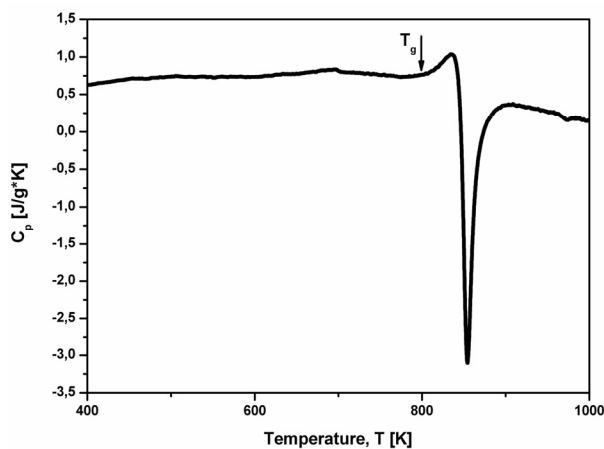


Fig. 11. The specific heat of  $\text{Fe}_{36}\text{Co}_{36}\text{B}_{19.2}\text{Si}_{4.8}\text{Nb}_4$  in form of rods with diameter of 2 mm in as-cast state (sample P3)



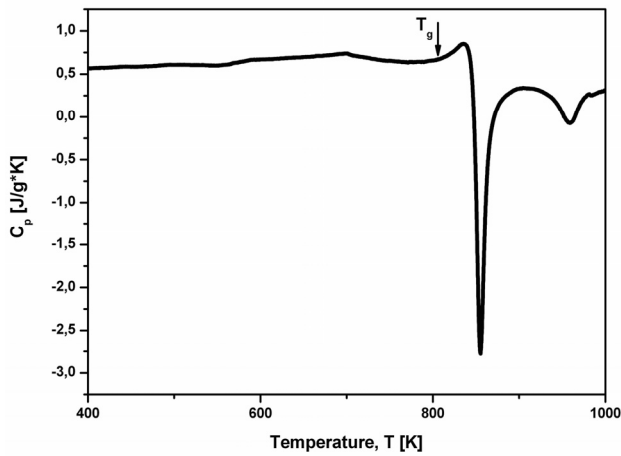


Fig. 12. The specific heat of  $\text{Fe}_{36}\text{Co}_{36}\text{B}_{19,2}\text{Si}_{4,8}\text{Nb}_4$  in form of rods with diameter of 2 mm in as-cast state (sample P4)

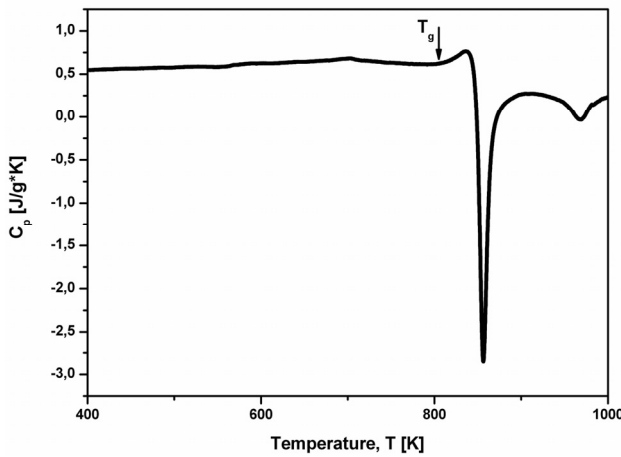


Fig. 13. The specific heat of  $\text{Fe}_{36}\text{Co}_{36}\text{B}_{19,2}\text{Si}_{4,8}\text{Nb}_4$  in form of rods with diameter of 2 mm in as-cast state (sample P5)

Above  $T_g$  specific heat insignificant increase but when the temperature reach  $T_x$ , although the heat was still supply into samples, growth of specific heat has not been observed. Above  $T_x$  it could be seen drastic decrease of  $C_p$ .

Table 6 presents values of specific heat dependence on glass transition temperature. Values were read from experimental data.

As it could be seeing for the samples with the same glass transition temperature the value of specific heat is different. This fact may be cause some changes in amorphous structure (atomic dense packing) of the samples.

Micrographs of fracture observations by scanning electron microscope were shown on Figs. 12-17. The changes of morphology are observable on the samples margin, mainly. The fracture surface is divided into two distinct regions: a smooth region and a vein pattern. The vein pattern occurs mostly because of sample local heating.

Cooling rate of metallic glasses is diversified on the cross section, and could be cause of temperature gradient. Gradient of

temperature may cause a thermal stresses in the consider region. As announce in [22] fracture morphology is connected with stress state in sample, also with the thermal stresses which could appear in material. Difference of fracture morphologies could be observed on the cross section of sample. In the edge, where sample had contact with copper mould morphology reveal veins fracture (Figs. 15, 17-20), in centre of samples it could be seen smooth fracture zone.

Table 6. Specific heat in glass transition temperature

No	$T_g$ [K]	$C_p$ [J/gK]
P1	806	0.914
P2	805	0.801
P3	805	0.765
P4	806	0.672
P5	806	0.625

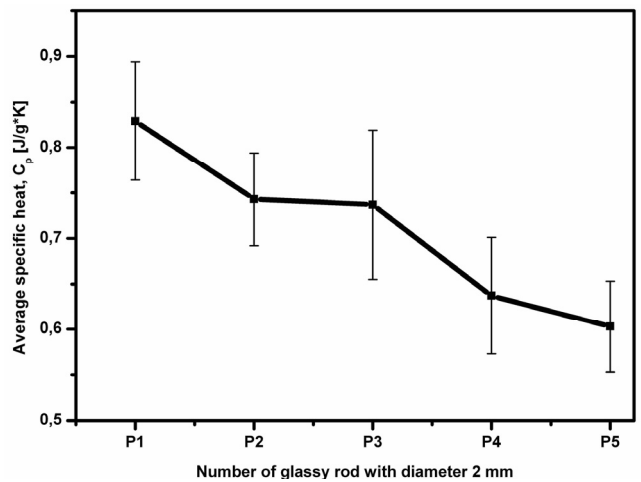


Fig. 14. Mean errors of specific heat results

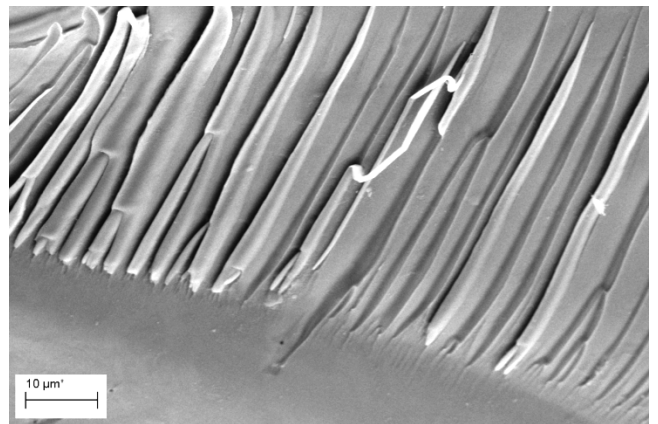


Fig. 15. SEM micrographs of the fracture morphology of  $\text{Fe}_{36}\text{Co}_{36}\text{B}_{19,2}\text{Si}_{4,8}\text{Nb}_4$  rod in as-cast state with diameter of 2 mm (4000x)

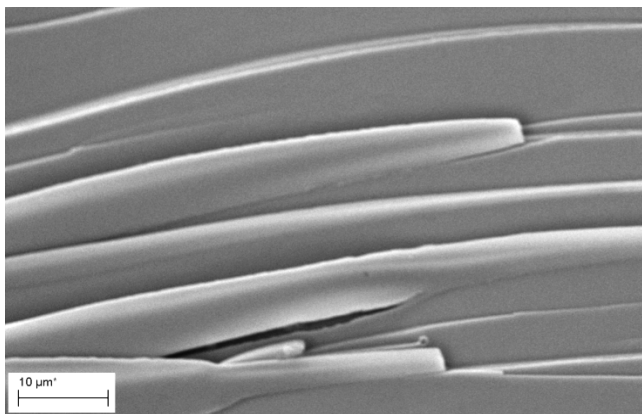


Fig. 16. SEM micrographs of the fracture morphology of  $\text{Fe}_{36}\text{Co}_{36}\text{B}_{19.2}\text{Si}_{4.8}\text{Nb}_4$  rod in as-cast state with diameter of 2 mm (5000x)

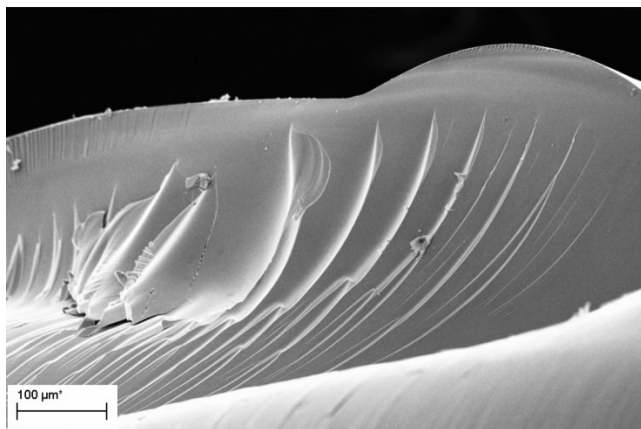


Fig. 19. SEM micrographs of the fracture morphology of  $\text{Fe}_{36}\text{Co}_{36}\text{B}_{19.2}\text{Si}_{4.8}\text{Nb}_4$  rod in as-cast state with diameter of 2 mm (500x)

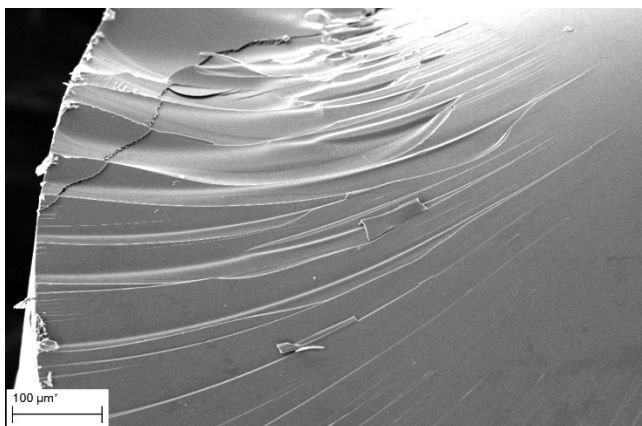


Fig. 17. SEM micrographs of the fracture morphology of  $\text{Fe}_{36}\text{Co}_{36}\text{B}_{19.2}\text{Si}_{4.8}\text{Nb}_4$  rod in as-cast state with diameter of 2 mm (500x)

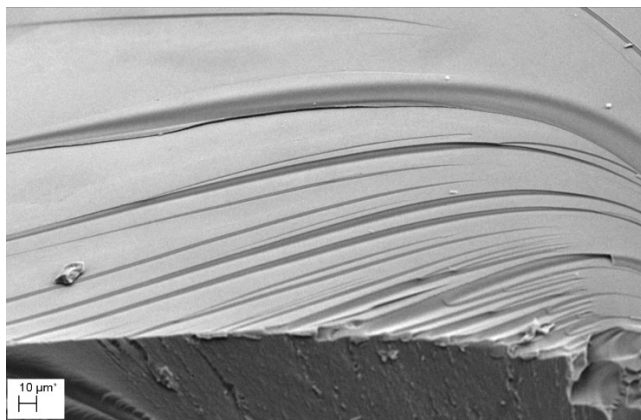


Fig. 20. SEM micrographs of the fracture morphology of  $\text{Fe}_{36}\text{Co}_{36}\text{B}_{19.2}\text{Si}_{4.8}\text{Nb}_4$  rod in as-cast state with diameter of 2 mm (1000x)

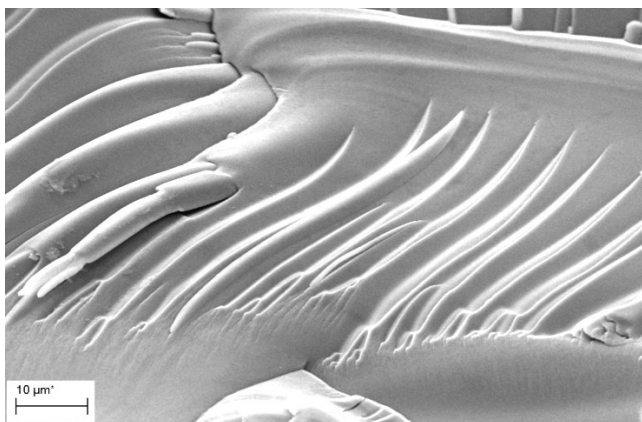


Fig. 18. SEM micrographs of the fracture morphology of  $\text{Fe}_{36}\text{Co}_{36}\text{B}_{19.2}\text{Si}_{4.8}\text{Nb}_4$  rod in as-cast state with diameter of 2 mm (4000x)

#### 4. Conclusions

Copper mould casting is effective technology of bulk metallic glasses fabrication. As it presented in paper,  $\text{Fe}_{36}\text{Co}_{36}\text{B}_{19.2}\text{Si}_{4.8}\text{Nb}_4$  bulk glassy rods could be obtained by this casting method.

Thermal properties of metallic glasses are very important issue for the sake of optimization of manufacturing process. Thermal conductivity and specific heat are significant properties in the point of view solidification and vitrification of molten alloy. The investigations performed on the samples of studied  $\text{Fe}_{36}\text{Co}_{36}\text{B}_{19.2}\text{Si}_{4.8}\text{Nb}_4$  bulk metallic glass in as cast state allowed to formulate the following statements:

- the DTA investigation enable to identification of melting point  $T_m = 1350$  K and liquidus  $T_l = 1434$  K temperatures,
- the X-ray diffraction revealed that the studied as-cast rods with diameter  $\phi=2$ mm were amorphous,

- DSC measurements allow to determinate glass transition temperature  $T_g = 805/806$  K, crystallization temperature: onset  $T_x = 840/842$  K and peak temperature  $T_p = 854/856$  K,
- the glass forming ability parameters such as  $T_{rg}$ ,  $\Delta T_x$ ,  $\alpha$ ,  $\beta$ ,  $\gamma$  could be also calculated,
- the specific heat investigations show that value of  $C_p$  is comparable for every five samples. For temperature range of 300 to 1000 K  $C_p$  average 0,829 J/g\*K for P1, 0,743 J/g\*K for P2, 0,686 J/g\*K for P3, 0,637 J/g\*K for P4 and 0,603 J/g\*K for P5,
- in the glass transition temperature it could be observed that  $C_p$  is different although the same value of  $T_g$ ,
- the changes in the amorphous structure (atomic dense packing) could have influence on the specific heat of bulk metallic glasses,
- the crystallization temperature, which is determinate by DSC measurement, cause drastic specific heat decrease of investigated metallic glasses,
- the SEM observations of investigated sample reveal various morphology: smooth regions and vein patterns,
- different morphology of examined bulk amorphous rods is probably result of changes in cooling rate on the sample cross section.

## References

- [1] R. Zallen, The physics of amorphous solids, Publishing House PWN, Warsaw, 1994 (in Polish).
- [2] W. Pilarczyk, R. Nowosielski, R. Babilas, P. Sakiewicz, A. Pilarczyk, Investigation of the structure and properties of Fe-Co-B-Si-Nb bulk amorphous alloy obtained by pressure die casting method, *Journal of Achievements in Materials and Manufacturing Engineering* 55/2 (2012) 363-367.
- [3] R. Nowosielski, A. Januszka, R. Babilas, Thermal properties of Fe-based bulk metallic glasses, *Journal of Achievements in Materials and Manufacturing Engineering* 55/2 (2012) 349-354.
- [4] R. Babilas, R. Nowosielski, Iron-based bulk amorphous alloys, *Archives of Materials Science and Engineering* 44/1 (2010) 5-27.
- [5] A. Januszka, R. Nowosielski, Structure and density of  $Fe_{36}Co_{36}B_{19.2}Si_{4.8}Nb_4$  bulk glassy alloy, *Journal of Achievements in Materials and Manufacturing Engineering* 52/2 (2012) 67-74.
- [6] A. Inoue, B.L. Shen, C.T. Chang, Fe- and Co-based bulk glassy alloys with ultrahigh strength of over 4000 MPa, *Intermetallics* 14 (2006) 936-944.
- [7] C. Suryanarayana, A. Inoue, Bulk metallic glasses, CRC Press, 2011.
- [8] W. Pilarczyk, The study of glass forming ability of Fe-based alloy for welding processes, *Journal of Achievements in Materials and Manufacturing Engineering* 52/2 (2012) 83-90.
- [9] R. Nowosielski, R. Babilas, A. Guwer, A. Gawlas-Mucha, A. Borowski, Fabrication of Mg65Cu25Y10 bulk metallic glasses, *Archives of Materials Science and Engineering* 53/2 (2012) 77-84.
- [10] S. Lesz, Preparation of Fe-Co-based bulk amorphous alloy from high purity and industrial raw materials, *Archives of Materials Science and Engineering* 48/2 (2011) 77-88.
- [11] A. Inoue, Bulk amorphous and nanocrystalline alloys with high functional properties, *Materials Science and Engineering A* 304-306 (2001) 1-10.
- [12] W.H. Wang, Roles of minor additions in formation and properties of bulk metallic glasses, *Progress in Materials Science* 52 (2007) 540-596.
- [13] M. Stoica, R. Li, A. R. Yavari, G. Vaughan, J. Eckert, N. Van Steenberge, D.R. Romera, Thermal stability and magnetic properties of FeCoBSiNb bulk metallic glasses, *Journal of Alloys and Compounds* 504S (2010) S123-S128.
- [14] Ch. Chang, B. Shen, A. Inoue, Synthesis of bulk glassy alloys in the (Fe,Co,Ni)-B-Si-Nb system, *Materials Science and Engineering A* 449-451 (2007) 239-242.
- [15] H.J. Sun, L. Li, Y.Z. Fang, J.X. Si, B. L. Shen, Bulk glassy  $(Fe_{0.474}Co_{0.474}Nb_{0.052})_{100-x}(B_{0.8}Si_{0.2})_x$  alloys prepared using commercial raw materials, *Journal of Non-Crystalline Solids* 358 (2012) 911-914.
- [16] C.A. Pampillo, A.C. Reimschuessel, The fracture topography of metallic glasses, *Journal of Materials Science* 9 (1974) 718-724.
- [17] B. Reinker, M. Dopfer, M. Moske, and K. Samwer, Specific heat of  $Zr_{65}Al_{7.5}Cu_{17.5}Ni_{10}$  around the glass transition, *The European Physical Journal B* 7 (1999) 359-364.
- [18] H.B. Ke, Z.F. Zhao, P. Wen, W.H. Wang, Specific heat in a typical metallic glass former, *Chinese Physics Letters* 29/4 (2012) 1-4.
- [19] Y. Tian, Z.O. Li, E. Yong Jiang, Low temperature specific heat and thermal conductivity of bulk metallic glass  $(Cu_{50}Zr_{50})_{94}Al_6$ , *Solid State Communications* 149 (2009) 1527-1530.
- [20] I.R. Lu, G.P. Gorler, H.J. Fecht, R. Willnecker, Investigation of specific heat and thermal expansion in the glass-transition regime of Pd-based metallic glasses, *Journal of Non-Crystalline Solids* 274 (2000) 294-300.
- [21] S.I. Abu-Eishah, Y. Haddad, A. Solieman, A. Bajbouj, A new correlation for the specific heat of metals, metal oxides and metal fluorides as a function of temperature, *Latin American Applied Research* 34 (2004) 257-265.
- [22] R.T. Qu, M. Stoica, J. Eckert, Z.F. Zhang, Tensile fracture morphology of bulk metallic glass, *Journal of Applied Physics* 108 (2010) 1-9.